Langmuir
Article
pubs.acs.org/Langmuir

Speciation of L-DOPA on Nanorutile as a Function of pH and Surface Coverage Using Surface-Enhanced Raman Spectroscopy (SERS)

Namhey Lee,*[†,‡] Daniel R. Hummer,[‡] Dimitri A. Sverjensky,[†,‡] Tijana Rajh,[§] Robert M. Hazen,[‡] Andrew Steele,[‡] and George D. Cody[‡]

[†]Department of Earth and Planetary Sciences, Johns Hopkins University, Baltimore, Maryland 21218, United States
[‡]Geophysical Laboratory, Carnegie Institution of Washington, Washington, D.C. 20015, United States
[§]Center for Nanoscale Materials, Argonne National Laboratory, Argonne, Illinois 60439, United States

Supporting Information

ABSTRACT: The adsorption configuration of organic molecules on mineral surfaces is of great interest because it can provide fundamental information for both engineered and natural systems. Here we have conducted surface-enhanced Raman spectroscopy (SERS) measurements to probe the attachment configurations of DOPA on nanorutile particles under different pH and surface coverage conditions. The Raman signal enhancement arises when a charge transfer (CT) complex forms between the nanoparticles and adsorbed DOPA. This Raman signal is exclusively from the surface-bound complexes with great sensitivity to the binding and orientation of the DOPA attached to the TiO_2 surface. Our SERS spectra show peaks that progressively change with pH and surface coverage, indicating changing surface speciation. At low pH and surface coverage, DOPA adsorbs on the surface lying down, with probably three points of attachment, whereas at higher pH and surface coverage DOPA stands up on the surface as a species involving two attachment points via the two phenolic oxygens. Our results demonstrate experimentally the varying proportions of the two surface species as a function of environmental conditions consistent with published surface complexation modeling. This observation opens up the possibility to manipulate organic molecule attachment in engineered systems such as biodetection devices. Furthermore, it provides a perspective on the possible role of mineral surfaces in the chemical evolution of biomolecules on the early Earth. Adsorbed biomolecules on mineral surface in certain configurations may have had an advantage for subsequent condensation reactions, facilitating the formation of peptides.

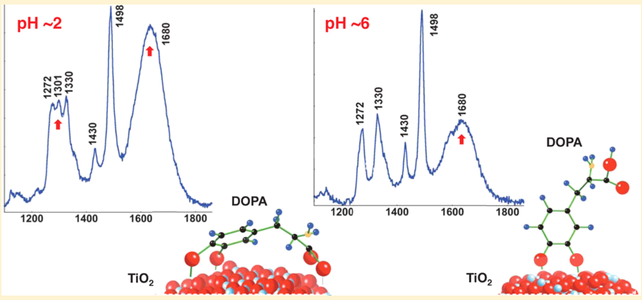

1. INTRODUCTION

The mechanism by which amino acids attach to mineral surfaces is important for understanding bioadhesion, biomineralization, and potentially the origin of life. One mechanism of bioadhesion occurs through proteins that contain the amino acid dihydroxyphenylalanine (DOPA).[1−4] This molecule is a member of the enediol family, which is also of great interest in the development of solar cells involving titanium dioxide and in biomedical imaging[5−7] because of the formation of a strong charge transfer complex when attached to nanosized semiconductor materials. In particular, our understanding of the mechanism of DOPA adsorption onto oxide surfaces as a function of environmental conditions is currently limited. In spite of the potential relevance, there are few experimental studies that have established the pH-dependent configuration of biomolecules at the mineral−water interface. There have been measurements of the adsorption of DOPA-like molecules such as catechol, dopamine, and 3,4-dihydroxyhydro hydrocinnamic acid (DHCA) using ATR-FTIR and surface-enhanced Raman spectroscopy (SERS), but under a limited range of environmental conditions.[8−11] Consequently, these studies observed only a single surface species, specifically one in which inner-sphere attachment occurs through the phenolic oxygens.

Measurements have been reported for DOPA adsorption on well-characterized rutile particles over a range of pH, ionic strength, and surface coverage and have been described using a surface complexation model establishing the stoichiometry, surface speciation, and thermodynamic equilibrium constants.[12] According to this model, at pH ~3 a DOPA species involving four attachment points ("lying down") is predominant, whereas at pH ~6 a species involving two attachment points via the phenolic oxygens ("standing up") predominates. The standing-up species is expected to be particularly important when DOPA is included as a constituent of proteins. This particular study also suggested that in the standing-up configuration (i.e., one strong bond and one weak one), DOPA may be able to "walk" across the rutile surface in water, which may help the development of reversible adhesives in water.[13−17] However, to date, there has been no direct experimental evidence of such surface species.

Received: September 7, 2012
Revised: November 14, 2012

Here, we studied the attachment modes of DOPA on nanorutile surfaces directly by using surface-enhanced Raman spectroscopy under a range of environmental conditions. It has been shown that certain molecule-functionalized metal oxide semiconductor nanoparticles exhibit enhanced Raman scattering.[11,18−20] This enhancement arises from the formation of a charge transfer (CT) complex between the nanoparticle and the molecule. This complex produces resonance Raman scattering when it absorbs light at the excitation frequency.[19] The signal is specific to the surface complex without detectible contributions from components/atoms of the substrate or the aqueous DOPA in the surrounding medium, providing an exceptional surface-specific method for studying how adsorption might change with environmental conditions. Below we report results that show directly how the pH and surface coverage affecting the configuration of surface complexes can be monitored with SERS.

2. MATERIALS AND METHODS

2.1. Nano-TiO_2 Preparation. A suspension of TiO_2 nanoparticles was prepared by the dropwise addition of titanium(IV) chloride (Alfa Aesar, 99.9%) to chilled deionized water.[21] Assuming that all hydrated Ti forms TiO_2, we calculated the concentration of TiO_2 to be 128 mM (10.3 g/L TiO_2). The initial crystallization product in this type of synthesis is normally anatase, which transforms to rutile over time.[22,23] Consequently, the solution was aged at 4 to 5 °C for 2 weeks for complete conversion to rutile while maintaining slow particle growth[21,22] prior to the adsorption experiments.

2.2. Experimental Procedure. All solutions were prepared using milli-Q water (millipore resistance 18.2 MΩ). DOPA (L-3,4-dihydroxyphenylalanine) was purchased from Acros Organics (99% purity). DOPA solutions were freshly prepared prior to each experiment. The DOPA solutions were sonicated for at least 20 min and visually checked prior to use in order to ensure complete dissolution. All solutions and samples containing DOPA were wrapped in aluminum foil in order to avoid degradation from exposure to light.

Suspensions of 10.3 g/L TiO_2 nanoparticles in water at pH ~1 were first sonicated to disperse the particles. Following this, known concentrations of DOPA were added. The pH was immediately adjusted to 2, 4, or 6 using aqueous NaOH. The highest pH studied was limited to 6 as DOPA tends to oxidize under higher-pH conditions.[12] In the case of the pH 6 solutions, two additions of NaOH were used as the pH is close to the point of zero charge (pH_{PZC}). First, the pH was increased substantially using concentrated NaOH (~10.3M), and then it was fine-tuned to pH ~6 using a more dilute solution (0.1 M). As soon as the DOPA was added to the TiO_2 suspension, an orange charge-transfer complex was observed. This orange color became more intense as the DOPA concentration increased. Once the solution was prepared, it was stored in a N_2 glovebox to inhibit DOPA oxidation prior to the Raman measurements. The suspensions containing the surface complexes were transferred to glass slides, each with a single-well depression. About 60 μL of the sample was transferred into the well and then covered with a glass coverslip. Raman measurements were performed less than half an hour after the samples were prepared. A total of 15 solutions were tested in this manner at pH values of ~2, 4, and 6 and at DOPA concentrations of 0.63, 3.12, 6.25, 12.5, and 25.0 mM at each pH. We kept the concentration of TiO_2 particles at 0.125 M.

2.3. Raman Measurements. Raman measurements were performed at the Center for Nanoscale Materials (CNM) at Argonne National Laboratory using confocal Raman spectroscopy and at the Geophysical Laboratory (GL), Carnegie Institution of Washington. Raman spectra were recorded using 514 nm laser excitation. The Raman setup at CNM employed a microscope-coupled spectrograph (Reinshaw inVia) and a Priceton Instruments Spec 10:400BR detector with Semrock filters for laser line filtering. Typical spectra acquisition parameters included 20 accumulations for 30 s, a 50× objective, and 4.4 mW laser power. Preliminary data were collected at the Geophysical Laboratory. The Raman setup at GL employed a Witec α-scanning near-field optical microscope that was customized to incorporate confocal Raman spectroscopic imaging. Objective lenses used included a ×100 LWD and a ×20 LWD with a 50 μm optical fiber. Spectra were collected on a Peltier-cooled Andor EMCCD chip after passing through a f/4 300 mm focal length imaging spectrometer. All spectra reported in the figures were measured at CNM.

3. RESULTS AND DISCUSSION

The rutile nanoparticles we synthesized consisted of pure rutile as confirmed by X-ray diffraction and were similar to previously synthesized samples using the same method.[22,23] A TEM image of the particles is shown in Figure 1S where, under dry condition, clusters of particles exist that appears to contain rods of about 10−20 nm in length and 5 nm in diameter. Assuming cylindrical rods of 10 nm length corresponds to a very approximate estimate of the surface area of about 53 $m^2\ g^{-1}$. Given the range of aqueous DOPA concentrations we used, from 0.63 to 25 mM, the maximum possible surface coverages (assuming 100% adsorption) range from 1.2 to 47 $\mu mols\ m^{-2}$. Previous batch adsorption measurements indicate much less than 100% adsorption and actual adsorption values of up to about 1.5 $\mu mols\ m^{-2}$ on a different sample of rutile.[12]

A representative spectrum is shown in Figure 1 for a pH of 6 at a DOPA concentration of 6.25 mM. This spectrum is almost identical to the published spectrum of dopamine (ref 11, Figure 1A). Consequently, we have adopted the same assignments for the major peaks seen under these particular conditions, as indicated in the summary in Figure 1. The close resemblance of the spectrum of dopamine suggest that at a pH of 6 the DOPA is standing up on the surface. The Raman enhancement derived from enediol molecules on the surface of TiO_2 nanoparticles is

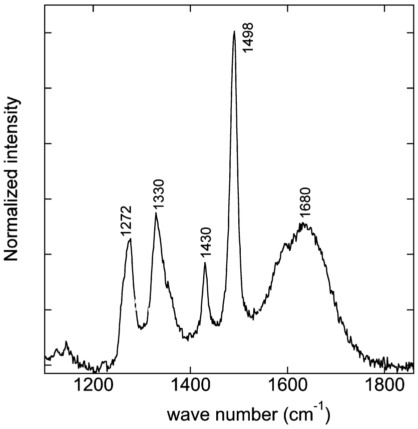

Peak assignments

Wave number (cm-1)	Vibrational assignment
1272	C-O from COOH or –NH3
1301	possibly COOH
1330	Aromatic
1430	C-H
1498	C=C aromatic
1680	Aromatic, C=O from COOH

Figure 1. Representative SERS spectra of DOPA on TiO_2, and 6.25 mM DOPA coverage at a pH of 6. This spectrum is almost identical to the dopamine on the TiO_2 spectrum in ref 11, indicating a similar adsorption configuration of DOPA on the TiO_2 surface through two phenolic oxygens.

about 1000.[24] The signal is exclusively from the surface-bound complex and, in particular, only those atoms of the ligands in immediate contact with the surface. Therefore, if the bound molecule changes its configuration (e.g., from "standing up" to "lying down"), then different parts of the molecular structure will contribute to the SERS spectrum. Consequently, the SERS signal becomes a highly sensitive in situ probe for the study of adsorption configurations. The Raman signals observed in this study were highly reproducible under all conditions and showed consistent results throughout the experiments.

3.1. Effect of pH. In spite of the importance of the organic–inorganic interface in water, our understanding of the pH dependence of adsorbed surface species of organic molecules on mineral surfaces is still in its early stages. The adsorption configuration of organic molecules is important as it can influence a number of fields such as the optimization of detection sensitivity in the development of biodetectors for imaging. In what follows, we first address how the adsorption properties of DOPA change with pH and examine the systematic changes in the SERS spectra. We also address how different functional groups preferentially interact with the surface as a function of pH by comparing the adsorption spectra of DOPA-like molecules from the enediol family.

3.1.1. Protonation Properties of Aqueous DOPA and TiO_2 and Predicted Surface Speciation of DOPA. The pH-dependent protonation states of aqueous DOPA are summarized in Figure 2a. Below a pH of about 2.2, DOPA is fully protonated and exists as a +1 cation. Between pH values of 2.2 and 8.8, DOPA exists in a zwitterionic form where the carboxylic group is deprotonated. Above a pH of 8.8, one hydroxyl group deprotonates, yielding a net charge of −1.[25]

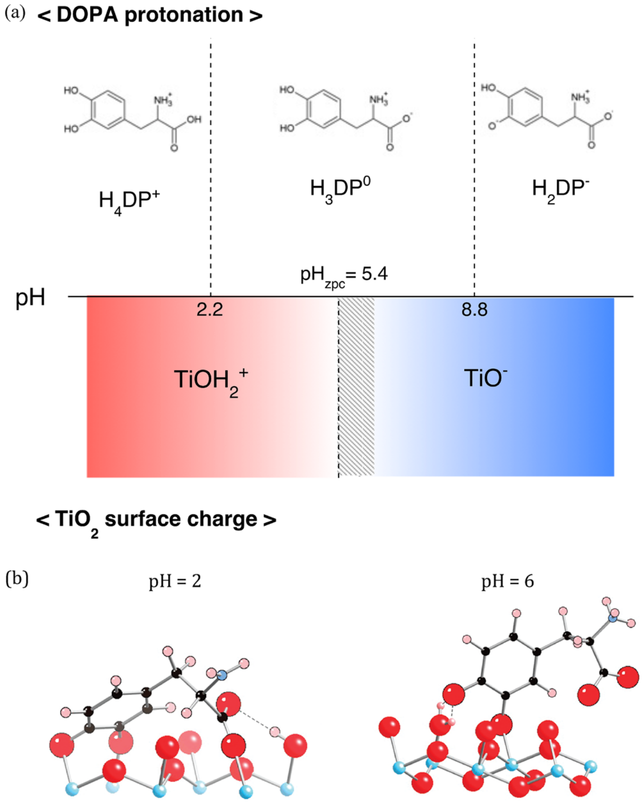

Figure 2. (a) Protonation properties of DOPA and TiO_2. (b) Previously proposed DOPA surface species as a functions of pH (ref 12).

We previously demonstrated that nanorutile powder has a point of zero charge of 5.4.[26] Therefore, below pH 5.4, the surface has more positively charged sites further away from the pH_{PZC} and vice versa for pH above 5.4 (Figure 2a). Although the TiO_2 particles (10−20 nm) that we used in the current study are smaller than those used for the pH_{PZC} measurement (100−400 nm), this value of pH_{PZC} is expected to be close, possibly a bit higher in pH. This is analogous to the studies of iron oxide nanoparticles whose point of zero charge tends to increase with decreasing particle size.[27]

Even though DOPA exists as a zwitterion between pH values of 2.2 and 8.8, bulk adsorption measurements show that it adsorbs strongly on rutile in this pH range.[12] Similarly, studies of the functionally related molecules catechol, dopamine, and hydrocinnamic acid also adsorb strongly in this pH range on oxide minerals. Furthermore, ATR-FTIR and SERS spectroscopic studies indicate that adsorption takes place through the phenolic oxygens.[8−11] On the basis of the protonation properties summarized above, it is conceivable that at low pH where the TiO_2 surface is largely positively charged, DOPA may have an additional interaction with the surface via the negatively charged COO− functional group, in addition to the two phenolic oxygen attachment points. Surface complexation modeling of the adsorption of DOPA on rutile is consistent with an expected change in surface speciation from lower to higher pH.[26] The two predicted model species are shown in Figure 2b. At low pH, DOPA was interpreted to be lying down on the surface attached through the phenolic oxygens and the carboxylate oxygens. In contrast, at higher pH DOPA was interpreted to be standing up on the surface, attached only through the phenolic oxygens.

3.1.2. pH Effect for Adsorbed DOPA on TiO_2. A strong pH effect is clearly shown in our spectra (Figure 3). As indicated above, at pH 6 our spectrum is essentially identical to that of dopamine on TiO_2. This strongly suggests that just like dopamine, DOPA is attached through the phenolic oxygens and is standing up on the surface (e.g., Figure 2b). As the pH decreases to 2, it can be seen in Figure 3a that the broad peak at about ∼1680 cm^{-1} increases significantly in intensity. Additionally, a new peak appears at about ∼1301 cm^{-1} that gradually grows in intensity with decreasing pH. These two distinctive changes can also be seen in Figure 3b where the spectra are superimposed. For other surface coverages, the response of the ∼1301 cm^{-1} peak was not so sensitive for the transition from pH 4 to 6, but there was always a distinctive difference when comparing pH 2 and 6 for all five surface coverage conditions (Figure 2S). These spectral changes indicate that at the lower pH values there is a change in the way that DOPA is attached to the surface compared to that at pH 6.

Because of the intrinsic complexity of a Raman signal involving even relatively simple organic molecules such as DOPA, we decided to use a simple ratio approach to quantify the changes in the 1301 and 1680 cm^{-1} peaks. We compared the changes in peak area by simply delineating the peaks at constant wavenumber limits (drop integration) and compared the peak areas at different experimental conditions after normalizing to the area of the 1498 cm^{-1} peak. The 1498 cm^{-1} peak was chosen for normalization because it is observed to respond consistently in relative intensity under the pH and surface coverage conditions. The calculated changes in the 1680/1498 and 1301/1498 area ratios are displayed in Figure 3c,d, respectively.

It can be seen in Figure 3c,d that the peak area ratios of 1301/1498 and 1680/1498 display some scatter as a function of pH, but overall they show systematic decreases with increasing

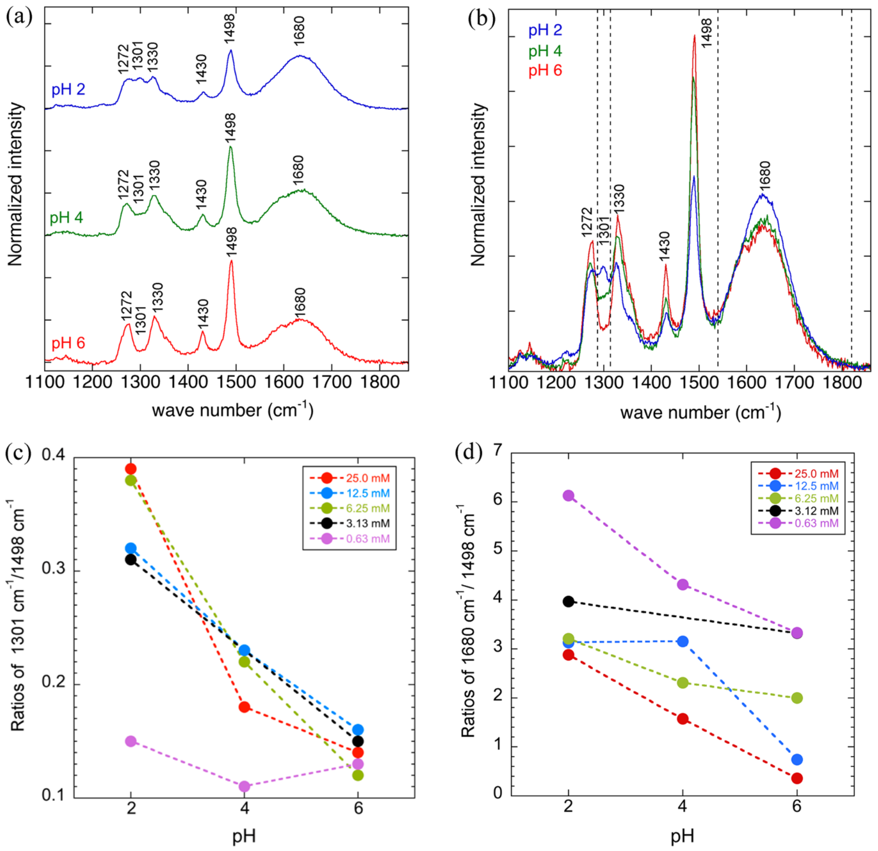

Figure 3. SERS spectra at pH values of 2, 4, and 6 with 6.25 mM DOPA loading showing changes in spectra with increasing pH. (a, b) As the pH increases, progressive reduction of the peaks at 1301 and 1680 cm^{-1} are observed. (c) Ratios of 1301/1498 cm^{-1} under the three pH conditions with varying DOPA concentrations. For all DOPA concentrations, as the pH increases from 2 to 6, the peak ratios gradually decrease. (d) Ratios of 1680/1498 cm^{-1} under the three pH conditions for varying DOPA concentrations. With increasing pH, the peak ratios decrease.

pH. The magnitudes of both of the peak ratios decrease from pH 2 to 6, consistent with what can be seen in the full spectra in Figure 3a,b. Again, this is consistent with a systematic change in the mode of attachment of the DOPA to the surface as a function of pH. An interpretation of these changes is discussed below.

3.2. Effect of Surface Coverage. In addition to pH effects, we also examined how the DOPA surface loading affects the Raman signal. When molecules are adsorbed on mineral surfaces more densely, it is possible that lateral interactions among the molecules or changes in the charge distribution at the interface could occur, leading to differences in adsorption configurations manifested by additional surface complexation reactions. In fact, in our previous study of batch adsorption of DOPA on TiO_2, it was predicted from the surface complexation modeling that with increasing surface coverage the DOPA attachment changed from "lying down" to "standing up".

It can be seen in Figure 4a that as more DOPA is adsorbed on the TiO_2 surface the Raman signals in the range of 1100 to 1540 cm^{-1} generally become stronger (although there is a minor reversal for 6.25 and 12.5 mM in the range from 1250 to 1350 cm^{-1}). However, at ~1680 cm^{-1} the exact opposite behavior is displayed. That is, as the surface coverage of DOPA increases, the peak size systematically decreases.

In Figure 4b, at pH 6, it can be seen that as the DOPA concentration increases, the spectra again show systematic and significant changes. Raman signals in the range of 1100 to 1540 cm^{-1} overall exhibit a stronger signal but without the 1301 cm^{-1} peak, as anticipated. In contrast, at ~1680 cm^{-1} the trend is exactly reversed, as for pH 2. At high surface coverage (e.g., 12.5 and 25 mM), the peak size reduction is very distinctive, again consistent with DOPA standing up on the surface at pH ~6 and high surface coverages. The decrease for the ~1680 cm^{-1} peak in Figure 4b is strong because it is favored both by the high pH (Figure 3b) and the high surface coverage.

The calculated changes in the 1680/1498 and 1301/1498 area ratios as a function of surface coverage at pH 2 and 6 are displayed in Figure 4c,d, respectively. First, it can be seen in Figure 4c that the ~1301 cm^{-1} peak shows a rather insensitive response to surface coverage changes. Increasing surface coverage results in a rather constant ratio for the 1301/1498 areas, except at low coverage at pH 2, where a different type of surface species is assumed. As for the 1680/1498 ratio, it shows a clear trend with increasing surface coverage. The ratio decreases, signifying more surface species standing up. This simple analysis highlights the overall changes in peak size as a function of pH and surface coverage.

Additionally, it can be seen in Figure 4b that two small, sharp peaks around 1580−1600 cm^{-1} appear at the highest surface coverages. These two peaks appeared only at pH 6 and high surface coverage. We speculate that these peaks originate from the lateral interactions of densely populated DOPA molecules on the rutile surface while the molecule is standing up on the surface.

3.3. Attachment Mechanisms. In this section, we interpret the above observations from a molecular point of view. It is well known that the two phenolic oxygens play a key role in the adsorption of molecules in the catechol family (Table 2).

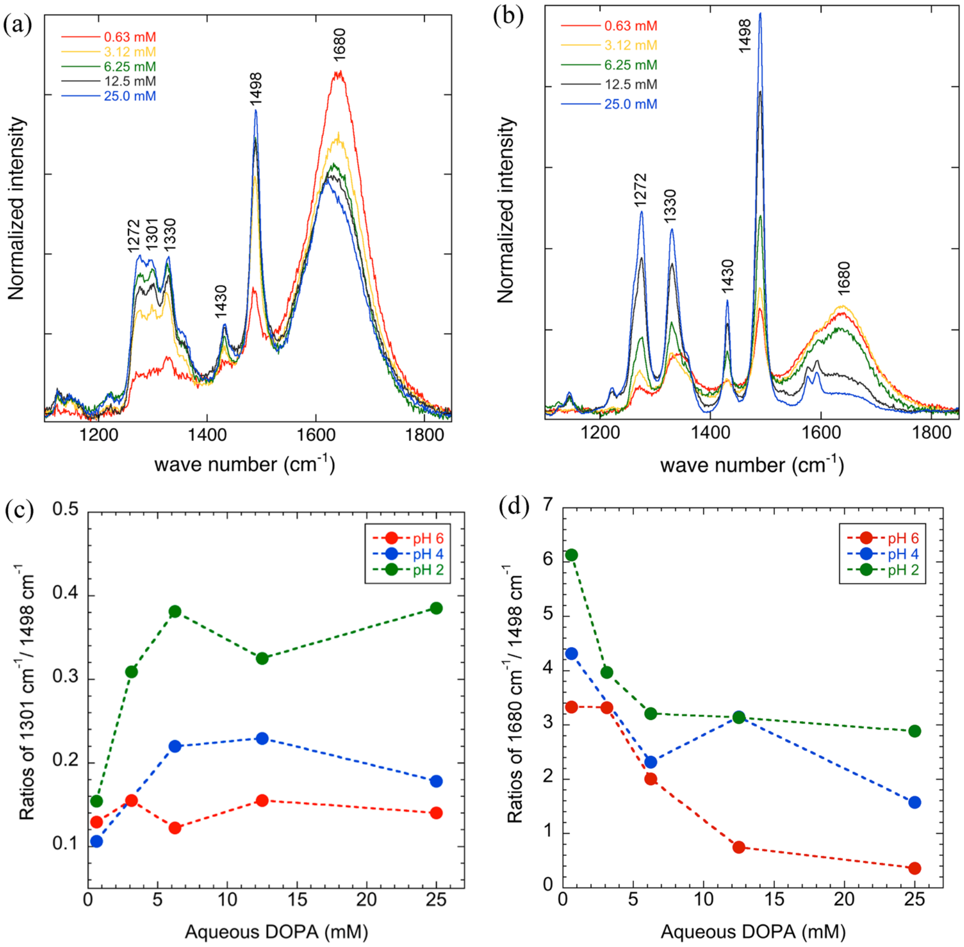

Figure 4. SERS spectra at DOPA concentrations of 0.63 to 25 mM. (a) At a pH of 2, the ~1680 cm^{-1} peak, where the vibration is mainly generated by the aromatic ring, decreases with increasing DOPA concentrations. This observation indicates that as the surface coverage increases, the interaction between the surface and aromatic ring become weaker. (b) At a pH of 6, similar changes occur, which is consistent with the standing-up species remaining dominant. (c) Peak ratio of 1301 cm^{-1}/1498 cm^{-1} as a function of DOPA surface coverage under different pH conditions. These peak ratios are relatively insensitive to surface coverage except for low pH conditions. (d) The peak ratio of 1680 cm^{-1}/1498 cm^{-1} decreases as a function of DOPA surface coverage, indicating a weaker interaction between the surface and the aromatic ring with increasing surface coverage.

Table 1. Chemical Structures of Enediol Molecules Considered in This Study

Chemical structure	Name
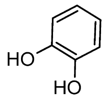	Pyrocatechol
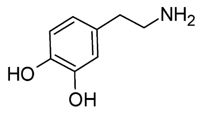	4-(2-aminoethyl) benzene-1, 2-diol (Dopamine)
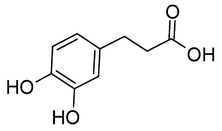	3,4-dihydroxylhydro cinnamic acid (DHCA)
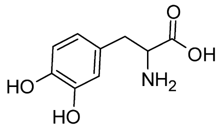	L-3,4-dihydroxyphenylalanine (DOPA)

As already indicated, at a pH of 6 the SERS spectrum contains peaks that are identical to those of previously published dopamine, which is known to adsorb standing up attached only by the phenolic oxygens. Consequently, it is clear that DOPA at

Table 2. End Member Analysis: Calculated Fractions of Surface Species for Each pH and DOPA Concentration

pH	25.0 mM		12.5 mM		6.25 mM		3.13 mM	
6	0.00	1.00	0.25	0.75	0.70	0.30	0.90	0.10
4	0.55	0.45	0.75	0.25	0.80	0.20	0.90	0.10
2	0.70	0.30	0.78	0.22	0.94	0.06	1.00	0.00
	lying down	standing up	lying down	standing up	lying down	standing up	lying down	standing up

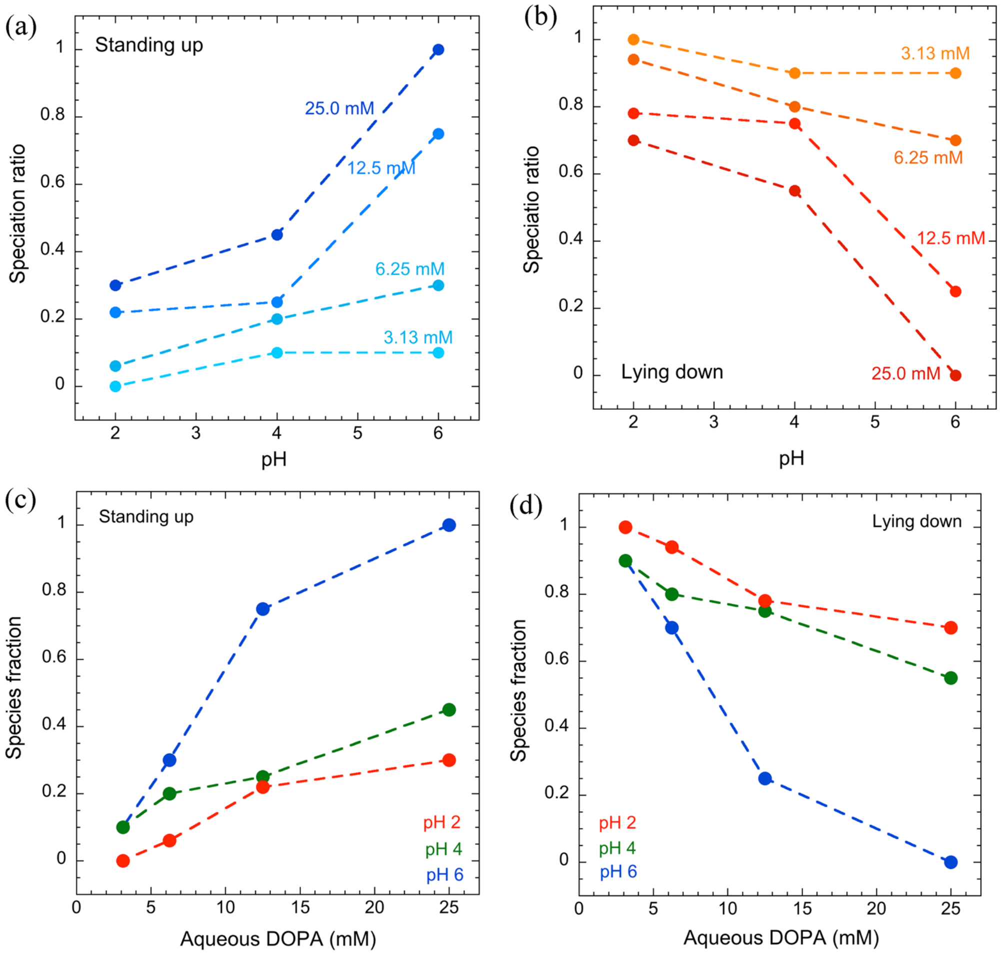

Figure 5. Calculated fractions of the two surface species as functions of pH and surface coverage based on the end-member analysis described in the text. (a) The fraction of standing-up species under different pH conditions for varying DOPA surface coverage. Generally, the fraction of standing-up species increases with increasing pH. For high-coverage conditions (e.g., 100 and 200%), the increase is more intense combined with the high-pH effect, where the standing-up species is already favored, as compared to lower-coverage conditions. (b) The fraction of lying-down species under different pH conditions for varying DOPA surface coverages. The fraction of lying-down species decreases with increasing pH. For high-surface-coverage conditions, the fraction decreases more drastically as compared to that for lower-surface-coverage conditions because of the combined effect of pH and surface coverage, both of which favor the standing-up species. (c, d) Surface speciation fractions expressed as a function of the surface coverage for each pH condition. As the surface gets more crowded, the fraction of standing-up species increases. Because of the combined pH and surface-coverage effects, at high surface coverage the trend is intensified.

a pH of 6 or at high surface coverage is also standing up on the surface. This surface species is consistent with the inference from surface complexation modeling (Figure 2b). However, at low pH, the systematic changes in the SERS spectra documented above strongly indicate that an alternate surface species dominates under these conditions.

At low pH, the principal changes in the SERS spectra involve the increased intensity of the 1680 cm^{-1} peak and the appearance of the 1301 cm^{-1} peak. The 1680 cm^{-1} peak mainly reflects the interaction between the aromatic ring and the TiO_2 surface. The increased intensity of this peak at low pH suggests that the aromatic ring is close to the surface in the attachment mode at pH 2. This is consistent with the DOPA molecule lying down on the surface. This observation is consistent for all surface coverage conditions.

The appearance of the 1301 cm^{-1} peak at low pH may indicate an additional interaction between DOPA and the surface. If DOPA lies down on the surface under these conditions, then the carboxylate of the DOPA or the protonated amine group ($-NH_3^+$) or both may interact with the rutile surface. In either case, this is consistent with the evidence from the 1680 cm^{-1} peak, as discussed above, that suggests that at low pH DOPA is lying down on the surface. Again, this is consistent with the previously published surface complexation modeling suggesting that DOPA molecules adsorb lying down on the surface at low pH. For example, the attachments shown in Figure 2b for DOPA lying down involve two phenolic oxygens involving Ti−O−C bonds and additional interactions via a Ti−O−C and a Ti−OH$_2$···O−C hydrogen bond, possibly via the deprotonated carboxylic group (COO$^-$).

To investigate this possibility further, we examined the Raman signals of other DOPA-like molecules adsorbed on nano-TiO$_2$ (Table 1) using previously published measurements at low pH values (∼1).[11] First, pyrocatechol, a benzene ring with two hydroxyl groups at the 3 and 4 positions and no other functional groups, is known to adsorb via the two hydroxyl groups. Its overall spectrum shows a very similar pattern to DOPA except that there is no sign of the peak at ∼1301 cm^{-1}. Similarly, the spectrum of dopamine, which has an amine group but no carboxylic group, also clearly lacks the 1301 cm^{-1} peak. The overall spectrum is very similar to that of pyrocatechol, slightly shifted to higher frequency and with a lower intensity. These observations suggest that the 1301 cm^{-1} peak in the DOPA spectra is coming from the carboxylic−surface interactions. This speculation is further supported by the spectrum of 3,4-dihydroxyhydro cinnamic acid (DHCA), which is structurally very similar to DOPA because it has a carboxylic group but no amine group. The spectrum of DHCA on TiO$_2$ clearly shows a 1301 cm^{-1} peak, albeit smaller than that for DOPA. Finally, a number of studies suggest that the amine group in amino acids does not interact with oxide surfaces; the interaction points are almost always via carboxylic groups.[26,28−32] These observations lead us to conclude that at low pH the DOPA molecules attach to the surface through the phenolic groups with an additional point of interaction that is most likely via the carboxylic group. This surface species appears to be favored at lower pH and under low surface coverage conditions.

In summary, we conclude that at low pH and low surface coverage DOPA molecules attach to the surface lying down approximately parallel to the surface with at least three points of attachment. At higher pH and higher surface coverage, DOPA attaches standing up, orthogonal to the surface, with two points of attachment via the two phenolic oxygens (Figure 2b). To be clear, two surface species are always present as surface complexes; only the ratios differ depending on the environmental conditions.

3.4. Distribution of Surface Species: End-Member Analysis.

To quantify the amounts of the two surface complex species as a function of pH and surface coverage, we attempted to fit our spectra using two end-member spectra and by assuming the additivity of the spectra. At a pH of 2 with 3.13 mM DOPA, we assumed that only the lying-down species contributes to the spectrum. At a pH of 6 with 25 mM DOPA, we assumed that only the standing-up species contributes to the spectrum. The proportions of each in the SERS spectra were adjusted to find the best fits. In most cases, a combination of the two end members fit the SERS spectra very satisfactorily (Figure 3S). The results are summarized in Table 2 and Figure 5.

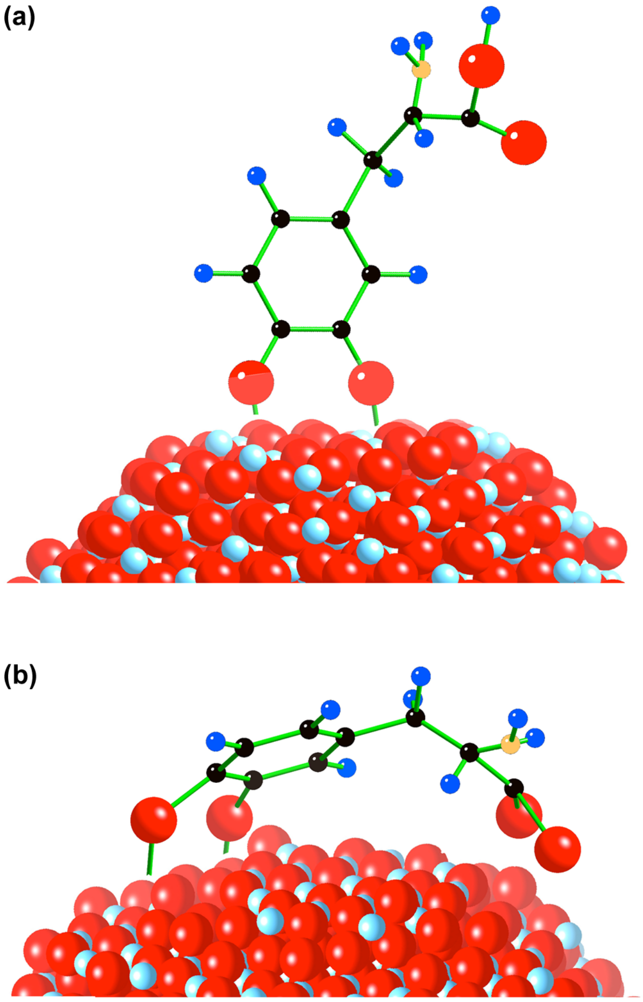

Figure 6. Proposed surface species of DOPA on a nanorutile particle. (a) Standing up orthogonal to the surface, with two points of attachment via the two phenolic oxygens. This species is favored at higher pH (∼6) and higher-surface-coverage conditions. (b) Lying-down species parallel to the surface possibly having at least three points of attachment. This species is favored at lower pH (∼2) and lower-surface-coverage conditions.

It can be seen in Figure 5 that the calculated fractions of two surface species vary significantly. In general, proportionally more lying-down species are observed at lower pH and lower surface coverage whereas standing-up species become more dominant at higher pH and higher-surface-coverage conditions. At a pH of 6, the combined pH and high-surface-coverage conditions favor a sharp increase in the standing-up species. At the same time, we observed a simultaneous sudden decrease in the lying-down species at pH ∼6 and a more smooth decrease under lower pH conditions (Figure 5a,b). When the species fractions are expressed as a function of coverage, the standing-up species increases with increasing coverage and the lying-down species decreases with increasing coverage. The combined effects of pH and surface coverage intensify the trends at higher pH and coverage as shown in Figure 5c,d.

4. CONCLUDING REMARKS

In summary, our SERS spectra clearly reveal the distinct binding and orientation of DOPA on the rutile (TiO$_2$) surface over a wide range of pH values and surface coverages. The data suggest that the surface-enhanced Raman spectra indicate the attachment mode of the molecules with high sensitivity to the environmental conditions. Two surface complex species are inferred to be present (Figure 6), and the proportions vary systematically depending on the experimental conditions.

The ability to characterize the orientation and binding mechanism of organic molecules at the mineral−water interface under in situ conditions has potential in a wide variety of applications. The systematic changes in the SERS spectra that we observed can potentially be adapted for the optimization of biodetection or biological recognition devices. Furthermore, the potential of having different modes of attachment under a given set of environmental conditions suggests the possibility of tuning certain chemical reactions. For example, under early Earth conditions, certain attachment modes of amino acids might have favored condensation reactions on mineral surfaces, thereby contributing to the evolution of primitive biomolecules.[31]

■ ASSOCIATED CONTENT

Ⓢ Supporting Information

TEM image of nanorutile. Additional spectra at different pH values and DOPA concentrations. Spectra of the two end-membered surface species and fits of the species to spectra measured under different conditions.This material is available free of charge via the Internet at http://pubs.acs.org.

■ AUTHOR INFORMATION

Corresponding Author

*E-mail: namheyl@jhu.edu.

Notes

The authors declare no competing financial interest.

■ ACKNOWLEDGMENTS

We greatly appreciate D. Gosztola and H. C. Fry at CNM for assistance with the Raman spectroscopy experiments. We also acknowledge B. Mysen for help with data analysis and discussion. K. Livi at Johns Hopkins University and T. Strobel at Carnegie Institution of Washington are gratefully acknowledged for performing TEM and XRD measurements, respectively. We thank M. Aihaiti for valuable discussions and Y. Mochizuki and C. Estrada for help in the laboratory and discussions. D.A.S. and N.L. express their appreciation for the facilities and hospitality extended to them by the Geophysical Laboratory of the Carnegie Institution of Washington. This research was conducted with support from the NSF EAR-1023865 (D.A.S.), DOE DE-FG02-96ER-14616 (D.A.S.), NSF EAR-1023889 (R.M.H.), NASA Astrobiology Institute, and the Carnegie Institution of Washington. Use of the Center for Nanoscale Materials was supported by the U.S. Department of Energy, Office of Science, Office of Basic Energy Science, under contract no. DE-AC02-06CH11357.

■ REFERENCES

(1) Guvendiren, M.; Brass, D. A.; Messersmith, P. B.; Shull, K. R. Adhesion of DOPA-functionalized model membranes to hard and soft surfaces. *J. Adhes.* **2009**, *85*, 631.

(2) Lin, Q.; Gourdon, D.; Sun, C. J.; Holten-Andersen, N.; Anderson, T. H.; Waite, J. H.; Israelachvili, J. N. Adhesion mechanisms of the mussel foot proteins mfp-1 and mfp-3. *Proc. Natl. Acad. Sci. U.S.A.* **2007**, *104*, 3782.

(3) Hwang, Y. S.; Liu, J.; Lenhart, J. J.; Hadad, C. M. Surface complexes of phthalic acid at the hematite/water interface. *J. Colloid Interface Sci.* **2007**, *307*, 124.

(4) Lee, H.; Scherer, N. F.; Messersmith, P. B. Single-molecule mechanics of mussel adhesion. *Proc. Natl. Acad. Sci. U.S.A.* **2006**, *103*, 12999.

(5) Li, S. C.; Wang, J. G.; Jacobson, P.; Gong, X. Q.; Selloni, A.; Diebold, U. Correlation between bonding geometry and band gap states at organic-inorganic interfaces: catechol on rutile $TiO_2(110)$. *J. Am. Chem. Soc.* **2009**, *131*, 980.

(6) Rajh, T.; Saponjic, Z.; Liu, J. Q.; Dimitrijevic, N. M.; Scherer, N. F.; Vega-Arroyo, M.; Zapol, P.; Curtiss, L. A.; Thurnauer, M. C. Charge transfer across the nanocrystalline-DNA interface: probing DNA recognition. *Nano Lett.* **2004**, *4*, 1017.

(7) Clarke, S. J.; Hollmann, C. A.; Zhang, Z. J.; Suffern, D.; Bradforth, S. E.; Dimitrijevic, N. M.; Minarik, W. G.; Nadeau, J. L. Photophysics of dopamine-modified quantum dots and effects on biological systems. *Nat. Mater.* **2006**, *5*, 409.

(8) Araujo, P. Z.; Morando, P. J.; Blesa, M. A. Interaction of catechol and gallic acid with titanium dioxide in aqueous suspensions. 1. Equilibrium studies. *Langmuir* **2005**, *21*, 3470.

(9) Gulley-Stahl, H.; Hogan, P. A.; Schmidt, W. L.; Wall, S. J.; Buhrlage, A.; Bullen, H. A. Response to "comment on surface complexation of catechol to metal oxides: an ATR-FTIR, adsorption, and dissolution study". *Environ. Sci. Technol.* **2010**, *44*, 6519.

(10) Lana-Villarreal, T.; Rodes, A.; Perez, J. M.; Gomez, R. A spectroscopic and electrochemical approach to the study of the interactions and photoinduced electron transfer between catechol and anatase nanoparticles in aqueous solution. *J. Am. Chem. Soc.* **2005**, *127*, 12601.

(11) Hurst, S. J.; Fry, H. C.; Gosztola, D. J.; Rajh, T. Utilizing chemical Raman enhancement: a route for metal oxide support-based biodetection. *J. Phys. Chem. C* **2011**, *115*, 620.

(12) Bahri, S.; Jonsson, C. M.; Jonsson, C. L.; Azzolini, D.; Sverjensky, D. A.; Hazen, R. M. Adsorption and surface complexation study of L-DOPA on rutile (α-TiO_2) in NaCl solutions. *Environ. Sci. Technol.* **2011**, *45*, 3959.

(13) Li, S. C.; Chu, L. N.; Gong, X. Q.; Diebold, U. Hydrogen bonding controls the dynamics of catechol adsorbed on a $TiO_2(110)$. *Surf. Sci.* **2010**, *328*, 882.

(14) Lee, H.; Lee, B. P.; Messersmith, P. B. A reversible wet/dry adhesive inspired by mussels and geckos. *Nature* **2007**, *448*, 338.

(15) Hamming, L. M.; Fan, X. W.; Messersmith, P. B.; Brinson, L. C. Mimicking mussel adhesion to improve interfacial properties in composites. *Compos. Sci. Technol.* **2008**, *68*, 2042.

(16) Lee, B. P.; Messersmith, P. B.; Israelachvili, J. N.; Waite, J. H.; Clarke, D. R.; Fratzl, P. Mussel-inspired adhesives and coatings. *Annu. Rev. Mater. Res.* **2011**, *41*, 99.

(17) Lau, K. H. A.; Ren, C.; Park, S. H.; Szleifer, I.; Messersmith, P. B. An experimental-theoretical analysis of protein adsorption on peptidomimetic polymer brushes. *Langmuir* **2012**, *28*, 2288.

(18) Musumeci, A.; Gosztola, D. J.; Schiller, T.; Dimitrijevic, N. M.; Mujica, V.; Marin, D.; Rajh, T. SERS of semiconducting nanoparticles (TiO_2 hybrid composites). *J. Am. Chem. Soc.* **2009**, *131*, 6040.

(19) Rajh, T.; Chen, L. X.; Lukas, K.; Liu, T.; Thurnauer, M. C.; Tiede, D. M. Surface restructuring of nanoparticles: an efficient route for ligand−metal oxide crosstalk. *J. Phys. Chem. B* **2002**, *106*, 10543.

(20) Tarakeshwar, P.; Finkelstein-Shapiro, D.; Rajh, T.; Mujica, V. Quantum confinement effects on the surface enhanced Raman spectra of hybrid systems molecule-TiO_2 nanoparticles. *Int. J. Quantum Chem.* **2011**, *111*, 1659.

(21) Kormann, C.; Bahnemann, D. W.; Hoffmann, M. R. Preparation and characterization of quantum-size titanium dioxide. *J. Phys. Chem.* **1988**, *92*, 5196.

(22) Li, G. S.; Li, L. P.; Boerio-Goates, J.; Woodfield, B. F. Grain-growth kinetics of rutile TiO_2 nanocrystals under hydrothermal conditions. *J. Mater. Res.* **2003**, *18*, 2664.

(23) Hummer, D. R.; Heaney, P. J.; Post, J. E. In situ observations of particle size evolution during the hydrothermal crystallization or TiO_2: a time-resolved synchrotron SAXS and WAXS study. *J. Cryst. Growth* **2012**, *344*, 51.

(24) Musumeci, A.; Gosztola, D.; Schiller, T.; Dimitrijevic, N. M.; Mujica, V.; Martin, D.; Rajh, T. SERS of semiconducting nanoparticles (TiO_2 hybrid composites). *J. Am. Chem. Soc.* **2009**, *131*, 6040.

(25) S Sanaie, N. H., C.A. Modeling l-dopa purification by chiral ligand-exchange chromatography. *AIChE J.* **2007**, *53*, 617.

(26) Jonsson, C. M.; Jonsson, C. L.; Sverjensky, D. A.; Cleaves, H. J., II; Hazen, R. M. Attachment of L-glutamate to rutile (α-TiO_2): a potentiometric, adsorption, and surface complexation study. *Langmuir* **2009**, *25*, 12127.

(27) Vayssieres, L. On the effect of nanoparticle size on water-oxide interfacial chemistry. *J. Phys. Chem. C* **2009**, *113*, 4733.

(28) Parikh, S. J.; Kubicki, J. D.; Jonsson, C. M.; Jonsson, C. L.; Hazen, R. M.; Sverjensky, D. A.; Sparks, D. L. Evaluating glutamate and aspartate binding mechanisms to rutile (r-TiO_2) via ATR-FTIR

spectroscopy and quantum chemical calculations. *Langmuir* **2011**, *27*, 1778.

(29) Jonsson, C. M.; Jonsson, C. L.; Estrada, C.; Sverjensky, D. A.; Cleaves, H. J., II; Hazen, R. M. Adsorption of L-aspartate to rutile (α-TiO_2): experimental and theoretical surface complexation studies. *Geochim. Cosmochim. Acta* **2010**, *74*, 2356.

(30) Roddick-Lanzilotta, A. D.; McQuillan, A. J. An in situ infrared spectroscopic study of glutamic acid and of aspartic acid adsorbed on TiO_2: implications for the biocompatibility of titanium. *J. Colloid Interface Sci.* **2000**, *227*, 48.

(31) Hazen, R. M.; Sverjensky, D. A. Mineral surfaces, geochemical complexities, and the origins of life. *Cold Spring Harbor Perspect. Biol.* **2010**, 2−21.

(32) Sverjensky, D. A.; Jonsson, C. M.; Jonsson, C. L.; Cleaves, H. J.; Hazen, R. M. Glutamate surface speciation on amorphous titanium dioxide and hydrous ferric oxide. *Environ. Sci. Technol.* **2008**, *42*, 6034.